Simulation-Based Evaluation of AC vs DC Electrodermal Activity Measurement Circuits for Long-Term Wearable Applications

Amir Mohammad Karimi Forood
Department of Biomedical Engineering
University of Connecticut
Storrs, Connecticut, USA
karimi@uconn.edu

Hugo F. Posada-Quintero
Department of Biomedical Engineering
University of Connecticut
Storrs, Connecticut, USA
hugo.posadaquintero@uconn.edu

***Abstract*— Electrodermal activity (EDA), an electrical manifestation of the sympathetic innervation of the sweat glands, is widely used in long-term physiological monitoring, including sleep, stress, and cognitive studies. DC-source devices are more commonly used for recording EDA due to their simplicity, while AC alternatives are less adopted because of their perceived complexity. However, maintaining low noise and ensuring signal stability over extended durations remains a significant challenge. This study uses LTspice simulations to compare AC and DC constant current EDA circuits under identical conditions. The electrode–skin interface is modeled using a Randles cell, and real EDA recordings are time-compressed to modulate tissue resistance. Results show that both AC and DC circuits perform comparably well in short-term recordings; however, over time, DC signals degrade due to electrode polarization in the Randles cell model, while AC remains stable and continues to capture EDA reliably.**

Keywords*— *Electrodermal Activity (EDA), LTspice Simulation, Signal Stability and Wearable Sensors

I. Introduction

Electrodermal activity (EDA) is a widely used biosignal for monitoring sympathetic nervous system activity and is increasingly applied in long-term contexts such as sleep research, mental health tracking, cognitive workload assessment, and ambulatory stress detection. These applications rely on stable, high-quality recordings with minimal noise or degradation, since robust signal processing and algorithm development depend on signals that accurately reflect physiological changes rather than artifacts caused by circuit limitations or variability at the electrode-skin interface[1].

EDA can be measured using either endosomatic or exosomatic methods. Endosomatic recordings detect spontaneous electrical potentials across the skin but are less commonly used due to their low amplitude and high susceptibility to noise. In contrast, exosomatic methods involve applying a small current through the skin and are more robust and better suited for continuous monitoring. This current can either be direct current (DC), which remains constant, or alternating current (AC), which oscillates sinusoidally. These approaches are known as DC-EDA and AC-EDA, respectively[2].

Research reported in this publication was supported by the National Institute of Diabetes and Digestive and Kidney Diseases of the National Institutes of Health under Award Number R01DK138248. The content is solely the responsibility of the authors and does not necessarily represent the official views of the National Institutes of Health.

During long-term use, the electrode–skin interface may introduce electrical instability, influenced in part by the type of excitation signal used. Comparing AC and DC excitation under these conditions helps clarify their respective strengths and limitations for wearable monitoring applications.

Although AC-EDA is theoretically more robust against these issues, no previous study has systematically compared the performance of AC and DC EDA circuits under identical conditions using both simulated and real EDA inputs. This study addresses that gap by conducting controlled LTspice simulations designed to evaluate the long-term performance of AC and DC excitation schemes using identical component values[2]. By using the same underlying circuit elements, the comparison remains unbiased, allowing the differences in performance to be attributed solely to the excitation method.

By using real EDA signals in this configuration, we can assess how effectively each circuit preserves the shape, amplitude, and dynamic range of the physiological signal. The simulated outputs are then compared with the original EDA data to evaluate which circuit configuration better maintains signal integrity over time.

Simulating the circuits over long durations also allows us to isolate the effects of the excitation type from other sources of variability, such as motion artifacts or environmental noise, which often confound experimental comparisons. In practice, maintaining stable long-term recordings is technically challenging and resource-intensive, making it difficult to attribute signal degradation solely to the excitation method. This fully controlled simulation environment, combined with the use of actual EDA recordings, provides a consistent physiological reference for precisely evaluating the signal fidelity of each circuit configuration.

II. Methods

To enhance simulation realism and ensure fair comparison between AC and DC excitation methods, we first mapped the Randles circuit components onto the skin's physiological layers to better reflect the electrode–tissue interaction (Fig. 1(a)). Based on this understanding, we developed a unified circuit model using a simplified version of the Randles cell by mirroring the dual-electrode interfaces into a single equivalent configuration, which includes time-varying tissue resistance and

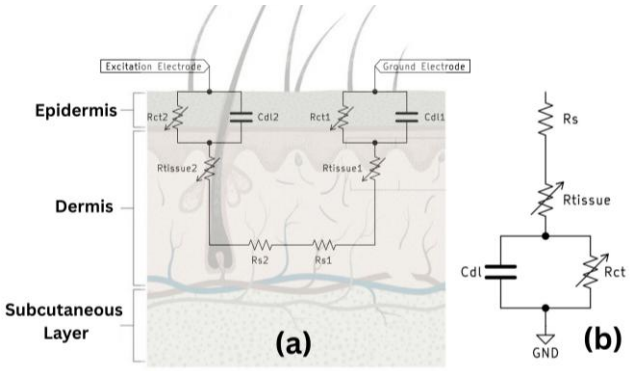

Fig. 1. Electrical model of the skin. (a) Randles cell components mapped onto skin anatomy. (b) Simplified Randles cell by mirroring electrodes into a single equivalent circuit.

polarization effects (Fig. 1(b)). Actual EDA recordings were used to dynamically modulate the tissue resistance within this model, enabling physiologically meaningful simulation conditions.

As the study adopts an exosomatic acquisition approach, current was delivered using a Howland current pump, which transforms an input voltage into a controlled current suitable for both AC and DC circuits (Fig. 2). Identical Howland pump configurations were applied in both setups to isolate the influence of the excitation type. The AC-EDA circuit was driven by a sinusoidal voltage input, while the DC-EDA circuit used a constant voltage source. All other circuit components, values, and structures were held constant.

Real EDA recordings from a public dataset were processed and streamed into LTspice to produce a long-duration waveform. This waveform was used to drive the R_{tissue} component of the model, providing a realistic testbed for circuit performance evaluation. Long-term simulations assessed signal fidelity under matched conditions for each excitation method.

A. Extended Randles Cell Model for Skin–Electrode Interface

The Randles model used in this study includes four key components that together represent the electrical behavior of the electrode–skin interface and the underlying tissue. R_s, the solution resistance, models the bulk resistance of the skin and subcutaneous tissue between the electrodes. It represents the passive path that current travels before reaching the active interface. R_{tissue}, placed in series after R_s, is a time-varying resistor derived from real EDA recordings.

C_{dl}, the double-layer capacitance, represents the charge accumulation at the boundary between the electrode and the skin. It simulates how ions in sweat respond to applied voltage by temporarily storing and releasing electrical charge. In parallel with C_{dl} is R_{ct}, the charge transfer resistance, which models the difficulty of ionic or electronic current crossing the electrode–skin barrier. In this simulation, R_{ct} gradually increases over time to reflect electrode polarization. This slow drift is applied under the same conditions in both DC-EDA and AC-EDA circuits to maintain consistency. Unlike the conventional Randles cell with fixed values, our model uses variable R_{tissue} and slowly changing R_{ct} to better reflect real physiological behavior in continuous EDA recordings[3].

B. Howland Current Pump

Since skin resistance (R_{tissue}) varies over time due to physiological responses, the current source must maintain consistent output despite these fluctuations to ensure signal accuracy during extended recordings[4].

To achieve this, we implemented a Howland current pump (Fig. 2). This circuit converts a differential voltage input into a constant current using an operational amplifier and a precisely matched resistor network. The Howland pump provides bidirectional current control and maintains high output impedance, making it suitable for both DC-EDA and AC-EDA configurations.

It is widely used in EDA systems due to its ability to deliver consistent current across varying skin impedance, reduce signal drift, and support compact, wearable hardware designs. Its precision and flexibility for both unidirectional and oscillatory signals made it ideal for this study. The output current of the Howland current pump is determined by the following equation:

$$Iout = \frac{Vsource}{R3} \tag{1}$$

The only difference between the two configurations lies in the type of voltage input. The AC-EDA circuit was driven by a 1 V, 75 Hz sinusoidal source, while the DC-EDA circuit used a constant 1 V DC source. All other aspects, including circuit schematics, component values, and configuration, remained identical.

C. Real-Time EDA Signal Streaming into LTspice

We used electrodermal activity (EDA) recordings from the Wearable Device Dataset from Induced Stress and Structured Exercise Sessions[5]. This dataset contains multiple short-term, high-quality EDA recordings collected with the Empatica E4 wristband at a sampling rate of 4 Hz.

Because capturing long-term signal variability was essential for evaluating the stability of both AC and DC excitation methods, we created a continuous 12.4-hour signal by concatenating EDA segments from multiple subjects. This approach helped generate a representative and uninterrupted waveform while minimizing the influence of subject-specific artifacts or poor-quality data.

The original EDA recordings were used to drive the R_{tissue} element in the simulation, allowing the circuit to reflect realistic variations in skin conductance over time. To make long-duration simulation feasible in LTspice, we compressed time by rescaling the original 4 Hz EDA signal to 512 Hz, representing a 125-fold increase in playback speed. This transformation enabled us to simulate only 350 seconds in LTspice while retaining the complete physiological variability and dynamics of the 12.4-hour recording. The R_{tissue} waveform was implemented in LTspice using the PWL file-based behavioral source, enabling frame-by-frame resistance updates during simulation using the Resource data file.

D. Voltage Measurement Method for EDA Extraction

To extract the EDA signal from both AC and DC circuits, voltage was measured across the time-varying resistor R_{tissue}. In the DC configuration, this voltage directly reflects EDA, as the applied current remains constant.

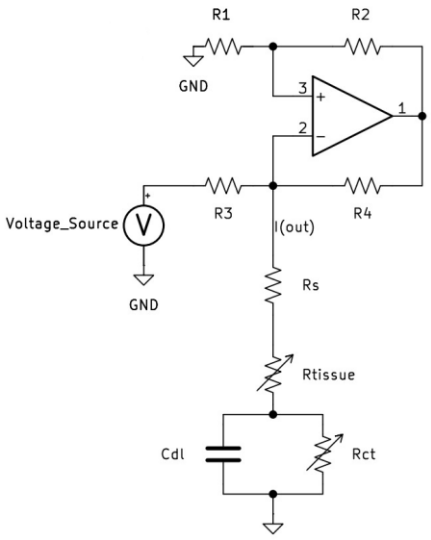

Fig. 2. The implemented Howland pump configuration used in this study, connected to the modified Randles cell to deliver a constant excitation current for both AC and DC simulations.

In the AC configuration, the voltage across Rtissue contains a high-frequency carrier modulated by slower physiological variations. To extract the EDA signal, we applied the Hilbert transform followed by a 4th-order zero-phase Butterworth low-pass filter with a 1 Hz cutoff. This removed the carrier while preserving low-frequency dynamics, resulting in a clean estimate of the EDA signal (Fig. 3)[6].

III. Results

We first compared the original EDA signal with the reconstructed signals from both AC-EDA and DC-EDA circuits. AC-EDA consistently tracks the shape and amplitude fluctuations of the original EDA trace across the full duration (Fig. 4(a)). In contrast, DC-EDA initially aligns well with the original signal but begins to diverge and degrade significantly in the latter part of the simulation, eventually collapsing to near-zero output (Fig. 4(b)).

Absolute error was computed as the difference between the reconstructed and original EDA signals at each time point. The resulting error plot shows that DC-EDA exhibits near-zero error during the early portion of the simulation, reflecting its initial high accuracy. However, as the simulation progresses and electrode polarization increases, DC-EDA accuracy deteriorates

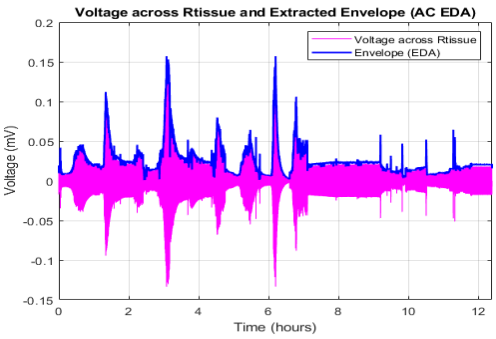

Fig. 3. Envelope extraction of AC-EDA voltage.

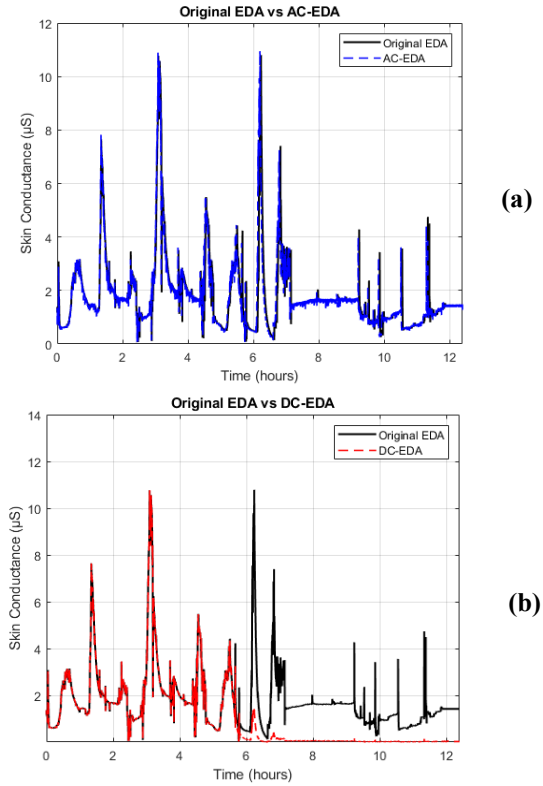

Fig. 4. Simulation of AC-EDA and DC-EDA over 12.4 hours. (a) AC-EDA vs. Original (b) DC-EDA vs. Original.

rapidly. Meanwhile, AC-EDA maintains a low and consistent error level throughout the entire simulation, with no signs of degradation (Fig. 5).

The current delivered through Rs (the Howland pump output) shows that in DC-EDA, the current eventually drops to zero due to the limitations of the Howland pump when driving a high-impedance load, indicating that the current source reaches its limit as polarization increases. Conversely, in AC-EDA, the sinusoidal excitation remains stable throughout the simulation (Fig. 6(a)).

The current through Cdl and Rct shows that in DC-EDA, no current passes through Cdl after a certain point, indicating halted capacitive behavior due to electrode polarization. (Fig. 6 (b-c)).

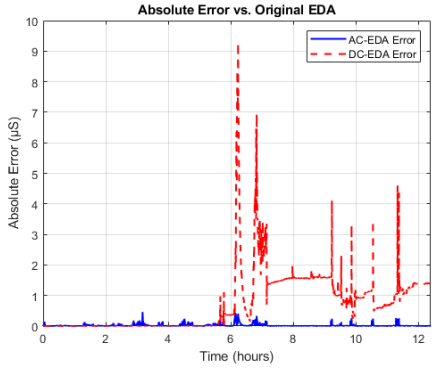

Fig. 5. Absolute error between original EDA and reconstructed signals from AC-EDA and DC-EDA.

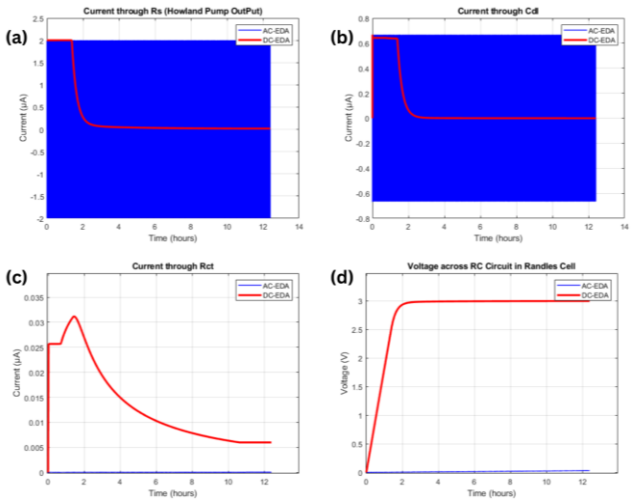

Fig. 6. Internal circuit behavior of the Randles model.

(a) Output Current of Howland Pump. (b) Current through $C_{dl.}$ (c) Current through $R_{ct.}$ (d) Voltage across the RC interface.

The voltage across the RC pair (R_{ct} and C_{dl}) in DC-EDA reveals increased charge buildup until it reaches capacitive saturation, while the AC-EDA circuit maintains small, sinusoidal fluctuations (Fig. 6(d)).

Quantitative metrics further highlight the comparative performance. Table I reports the Pearson correlation, mean absolute error (MAE), and signal-to-noise ratio (SNR) for both the short-term period before DC-EDA failure and the full 12.4-hour duration.

TABLE I. STATISTICAL COMPARISON OF AC-EDA AND DC-EDA PERFORMANCE

METRIC	AC-EDA (BEFORE DC FAILURE)	DC-EDA (BEFORE DC FAILURE)	AC-EDA (FULL DURATION)	DC-EDA (FULL DURATION)
P[a]	0.9725	1.000	0.9347	0.7755
MAE[b] (μS)	0.0173	0.0021	0.0201	0.7387
SNR[c] (dB)	37.22	58.91	33.09	5.38

[a.] P: Pearson correlation coefficient.

[b.] MAE: Mean Absolute Error.

[c.] SNR: Signal-to-Noise Ratio.

IV. DISCUSSION

While many experts recommend using AC-EDA to avoid polarization issues associated with DC-EDA, the literature has lacked direct evidence comparing their long-term behaviors. This study provides the first clear demonstration of DC-EDA degradation over time and validates the reliability of AC-EDA under identical physiological input. This simulation reveals a key trade-off between DC-EDA's short-term accuracy and AC-EDA's long-term reliability. DC-EDA initially reconstructs the EDA signal with perfect fidelity, but its performance declines steadily due to electrode polarization. This leads to a collapse in signal amplitude, increased absolute error, current source saturation, and distortions in the RC interface.

AC-EDA, by contrast, maintains stable performance throughout the full simulation. While its initial error is slightly higher than DC-EDA, it avoids the cumulative charge buildup that causes DC drift. Its sinusoidal excitation periodically discharges interface components like C_{dl} and R_{ct}, preventing long-term distortion. As a result, AC-EDA sustains high correlation with the original signal over time.

The trends observed in current and voltage signals across internal circuit elements, along with the summary in Table I, reinforce these findings. DC-EDA starts slightly ahead in all metrics, but its performance collapses as polarization increases. This is evident in dropping correlation, rising error, and reduced SNR. Eventually, the Howland pump fails to drive the load, delivering zero current as impedance increases, while the RC interface becomes fully polarized[7]. In contrast, AC-EDA keeps both current and voltage within expected ranges, demonstrating better handling of prolonged physiological input.

V. CONCLUSION

While DC-EDA may be suitable for brief, controlled sessions, AC-EDA proves to be significantly more robust for continuous, long-term monitoring especially in wearable devices where real-time recalibration is not feasible. For applications requiring signal stability and minimal maintenance, AC-EDA presents a clear and practical advantage.

REFERENCES

[1] H. F. Posada-Quintero, T. Dimitrov, A. Moutran, S. Park, and K. H. Chon, "Analysis of Reproducibility of Noninvasive Measures of Sympathetic Autonomic Control Based on Electrodermal Activity and Heart Rate Variability," *IEEE Access*, vol. 7, pp. 22523–22531, 2019, doi: 10.1109/access.2019.2899485.

[2] W. Boucsein, *Electrodermal Activity*. Boston, MA: Springer US, 2012. doi: 10.1007/978-1-4614-1126-0.

[3] H. S. Magar, R. Y. A. Hassan, and A. Mulchandani, "Electrochemical Impedance Spectroscopy (EIS): Principles, Construction, and Biosensing Applications," *Sensors*, vol. 21, no. 19, p. 6578, Oct. 2021, doi: 10.3390/s21196578.

[5] A. Hongn, F. Bosch, L. E. Prado, J. M. Ferrández, and M. P. Bonomini, "Wearable Physiological Signals under Acute Stress and Exercise Conditions," *Sci. Data*, vol. 12, no. 1, Mar. 2025, doi: 10.1038/s41597-025-04845-9.

[6] H. F. Posada-Quintero and K. H. Chon, "Innovations in Electrodermal Activity Data Collection and Signal Processing: A Systematic Review," *Sensors*, vol. 20, no. 2, p. 479, Jan. 2020, doi: 10.3390/s20020479.

[7] A. Mahnam, H. Yazdanian, and M. Mosayebi Samani, "Comprehensive study of Howland circuit with non-ideal components to design high performance current pumps," *Measurement*, vol. 82, pp. 94–104, Mar. 2016, doi: 10.1016/j.measurement.2015.12.044.